



## RESEARCH ARTICLE

10.1029/2022MS003460

## Understanding Precipitation Bias Sensitivities in E3SM-Multi-Scale Modeling Framework From a Dilution Framework

Nana Liu<sup>1</sup> , Michael S. Pritchard<sup>1,2</sup> , Andrea M. Jenney<sup>1</sup> , and Walter M. Hannah<sup>3</sup> <sup>1</sup>Department of Earth System Science, University of California, Irvine, CA, USA, <sup>2</sup>NVIDIA Research, Santa Clara, CA, USA, <sup>3</sup>Lawrence Livermore National Laboratory, Livermore, CA, USA

## Key Points:

- Dimensionality of cloud-resolving models in the Energy Exascale Earth System Model Multi-scale modeling framework (MMF) exhibits a striking effect on mean state precipitation patterns in subregions of the tropics
- MMFs tend to produce too many precipitating events but the use of 3D leads to fewer and is associated with an enhanced dilution in 3D
- Fast precursors of these climatological sensitivities are found that point to calibration targets for convection permitting global models

## Supporting Information:

Supporting Information may be found in the online version of this article.

## Correspondence to:

N. Liu,  
[nana.liu@uci.edu](mailto:nana.liu@uci.edu)

## Citation:

Liu, N., Pritchard, M. S., Jenney, A. M., & Hannah, W. M. (2023). Understanding precipitation bias sensitivities in E3SM-multi-scale modeling framework from a dilution framework. *Journal of Advances in Modeling Earth Systems*, 15, e2022MS003460. <https://doi.org/10.1029/2022MS003460>

Received 25 OCT 2022

Accepted 17 MAR 2023

**Abstract** We investigate a set of Energy Exascale Earth System Model Multi-scale modeling framework (MMF) (E3SM-MMF) simulations that vary the dimensionality and momentum transport configurations of the embedded cloud-resolving models (CRMs), including unusually ambitious 3D configurations. Issues endemic to all MMF simulations include too much Intertropical Convergence Zone rainfall and too little over the Amazon. Systematic MMF improvements include more on-equatorial rainfall across the Warm Pool. Interesting sensitivities to the CRM domain are found in the regional time-mean precipitation pattern over the tropics. The 2D E3SM-MMF produces an unrealistically rainy region over the northwestern tropical Pacific; this is reduced in computationally ambitious 3D configurations that use 1,024 embedded CRM grid columns per host cell. Trajectory analysis indicates that these regional improvements are associated with desirably fewer tropical cyclones and less extreme precipitation rates. To understand why and how the representation of precipitation improved in 3D, we propose a framework that dilution is stronger in 3D. This viewpoint is supported by multiple indirect lines of evidence, including a delayed moisture-precipitation pickup, smaller precipitation efficiency, and amplified convective mass flux profiles and more high clouds. We also demonstrate that the effects of varying embedded CRM dimensionality and momentum transport on precipitation can be identified during the first few simulated days, providing an opportunity for rapid model tuning without high computational cost. Meanwhile the results imply that other less computationally intensive ways to enhance dilution within MMF CRMs may also be strategic tuning targets.

**Plain Language Summary** The resolution of current climate models is not sufficient to resolve cloud and convective processes. Global cloud-resolving models (CRMs) have resolutions fine enough to represent individual cloud events but require too much computing power to be practical for large ensemble multi-decadal climate projection. Multi-scale modeling framework (MMF) is used to simulate climate by embedding thousands of small CRMs interactively in each grid column of a planetary model. Trade-offs in CRM configurations can influence the resulting emergent behavior. To examine this issue, we explore the effects of unusually ambitious 3D CRM configurations. Results show some interesting differences in the regional precipitation over the tropics. The 2D MMF produces an unrealistically rainy region over the northwestern tropical Pacific. Such biases are significantly reduced in 3D due to fewer tropical cyclones. To understand why and how the representation of precipitation improved in 3D, we propose a framework in which mixing being stronger in 3D is a major part of the story. This favored explanation is hard to prove directly but a few lines of circumstantial evidence support the case. Additionally, rapid effects of mixing that is seen in the first few days of global cloud resolving simulations provide opportunities for optimizing longer-term statistics.

## 1. Introduction

Precipitation is a fundamental component of the Earth system, linked to clouds, moisture transport, and the global atmospheric circulation via latent heat release. Extreme precipitation events, for example, hurricanes, floods, and droughts, can be life-threatening, and often lead to extensive socioeconomic losses. A number of studies have suggested that precipitation intensity will increase as atmospheric moisture increases under a warming climate (Allen & Ingram, 2002; Donat et al., 2016; Norris et al., 2019; Sun et al., 2007; Trenberth et al., 2003). Despite the socioeconomic importance of precipitation, the correct representation of precipitation is still a challenging task in climate models. Therefore, accurate knowledge of precipitation and how it can be realistically simulated is essential for understanding global and regional water and energy balances.

© 2023 The Authors. Journal of Advances in Modeling Earth Systems published by Wiley Periodicals LLC on behalf of American Geophysical Union. This is an open access article under the terms of the [Creative Commons Attribution License](https://creativecommons.org/licenses/by/4.0/), which permits use, distribution and reproduction in any medium, provided the original work is properly cited.

Global climate models (GCMs) capably simulate many features of the climatological spatial pattern of precipitation, although sometimes due to an incorrect combination of precipitation frequency and intensity (Dai et al., 1999; Sun et al., 2007). It has been reported that GCMs tend to produce an unrealistically high precipitation frequency but low intensity, even though precipitation amounts are realistic (Dai & Trenberth, 2004; DeMott et al., 2007; Zhou et al., 2008). Dai (2006) and Huang et al. (2017) also suggested that extreme precipitation is generally underestimated in most climate models. This is not surprising since precipitation is a result of processes that are mostly parameterized in current climate models, a difficult task due to their complexity. For example, cloud organization at mesoscales (Houze, 2004) can account for much of the Earth's precipitation and produce severe weather events and flooding. Y. Lin et al. (2017) and Moncrieff et al. (2017) suggested that the conspicuous summer warm and dry bias over the central United States in one climate model is associated with the failure of that climate model in simulating mesoscale convective systems. However, no existing GCMs include a satisfactory parameterization of mesoscale cloud circulation. In other words, current climate models still have room for improvement in simulating precipitation processes and a deeper understanding is needed to accurately depict important mechanisms driving precipitation changes.

Cloud resolving models (CRMs) are attractive as they have resolutions fine enough to represent individual cloud circulations, providing a wealth of information on cloud processes. While such models can be run globally for multiple months (Stevens et al., 2019) this is still impractical for the multi-decadal simulations required for most numerical climate science, pending additional increases in computing power or the capacity to better exploit it. Meanwhile, another promising approach to improve the representation of these small-scale processes is to use super-parameterization (SP), better known as the multi-scale modeling framework (MMF) approach to climate simulation, where the convective parameterization in the GCM is replaced with a small, laterally periodic, and usually two dimensional (2D) CRM domain in each GCM grid column (Grabowski, 2001; Grabowski & Smolarkiewicz, 1999; M. Khairoutdinov et al., 2005; Randall et al., 2003). While not without its own limitations, MMF has shown significant improvement in simulating precipitation variability and statistics, such as the diurnal cycle of precipitation (M. Khairoutdinov et al., 2005; Pritchard et al., 2011), regional mesoscale convective system properties (L. Lin et al., 2021; Pritchard et al., 2011; K. Zhang et al., 2017), and rainfall intensity and extreme precipitation (Demott et al., 2007; Kooperman et al., 2016; Li et al., 2012). Furthermore, a number of studies have demonstrated the ability of MMF to improve intraseasonal-to-seasonal scale variability, such as the Madden-Julian oscillation (Benedict & Randall, 2009), the South Asian Monsoon (Krishnamurthy et al., 2014), and the El Niño Southern Oscillation (Stan et al., 2010).

The MMF strategy discussed herein can be used with either 2D or 3D embedded CRMs in each GCM grid cell. In the classical 2D MMF, one issue is how to align the subgrid model within each large-scale model (i.e., east-west or north-south). Tulich (2015) suggested that tropical rainfall bias can be sensitive to the choice of CRM orientation. M. Khairoutdinov et al. (2005) suggested that the simulations based on the 2D MMF tend to produce an unrealistically humid and rainy region over the tropical western Pacific during the boreal summer, which was partially reduced through the use of the 3D MMF.

As the MMF approach exits its infancy and begins to be explored for potential operational use by major climate modeling centers (W. M. Hannah et al., 2020) it is important to understand the physical underpinnings of these chronic rainfall biases. Given their unique positioning to simulate climate with an approximation of convective processes that involves fewer assumptions relative to models with parameterized convection, a well-tuned MMF could be of interest for making climate predictions complementary to standard CMIP6 models.

But tuning MMF rainfall is an unfamiliar art especially regarding the novel knobs of CRM grid structure, dimensionality and formulation of momentum feedback. Currently, it is not clear why applying a 3D embedded model, which requires much more computational cost than a 2D embedded model and thus trades off against important throughput and cost constraints, can be useful to reduce the large precipitation bias over the tropical northwestern Pacific. Another under-explored issue is the effect of convective momentum transport (CMT), which on the one hand can impact the mean climate and the intraseasonal variability (Deng & Wu, 2010; Kim et al., 2008; Richter & Rasch, 2008; Wu & Yanai, 1994) but on the other hand is typically neglected in the implementation of most 2D versions of SP GCMs.

In this context, the goal of this study is to investigate the effects of varying embedded CRM dimensionality and momentum transport on the simulated precipitation in a state-of-the-art SP model. Practically, we hope to understand how to optimize the representation of tropical mean climate and its variability in MMFs. In the process, we

seek new insight into the multi-scale physics that produce these emergent effects on the planetary water cycle, where the causality can become complicated when convection is made explicit.

The rest of this paper is organized as follows. Section 2 describes the simulations and observational data. We begin by comparing the climatology of seasonal precipitation climatology across MMF configurations and observations in Section 3.1, followed by a trajectory analysis of precipitating events to understand variability behind the time mean in Section 3.2. Then, Section 3.3 formulates a hypothetical explanation for a striking effect of dimensionality on the mean precipitation pattern. Sections 3.4 and 3.5 present supporting evidence for the hypothesis. Finally, Section 4 draws the conclusion and discusses the potential application and limitations of our results.

## 2. Data and Method

### 2.1. Model Simulations

The Energy Exascale Earth System Model MMF (E3SM-MMF) is a climate model, originally adapted from the SP Community Atmosphere Model (SP-CAM; M. Khairoutdinov et al., 2005), in which a CRM, here the System for Atmosphere Modeling (M. F. Khairoutdinov & Randall, 2003), is embedded within each grid cell of the E3SM atmosphere model (EAM; Rasch et al., 2019). In the conventionally parameterized EAM, turbulence, shallow cumulus cloud, and stratocumulus cloud are parameterized using the Cloud Layer Unified by Binormals (CLUBB) parametrization (Bogenschutz et al., 2013; Golaz et al., 2002). Deep convection is based upon the Zhang-McFarlane (ZM) scheme (G. J. Zhang & McFarlane, 1995) and cloud microphysics is parameterized using Morrison and Gettelman (MG2; Gettelman et al., 2015). Aerosol concentration and sea surface temperature are prescribed with present-day values. In the E3SM-MMF the convection and boundary layer turbulence parameterizations are replaced by embedded CRMs whose grid structure is not constrained by the grid spacing of the host GCMs. For 2D CRM configurations we use 32 CRM grid columns aligned in the north-south direction while the 3D has  $32 \times 32$  grid columns with a grid spacing of 2 km. More details of the E3SM-MMF can be found in W. M. Hannah et al. (2020). All configurations of this study use a spectral element dynamical core on a cubed sphere geometry with 45 elements along each cube edge (ne45). Physics calculations, including the CRM of E3SM-MMF, are performed on a finite volume grid with  $2 \times 2$  cells per element (ne45pg2). The physics grid is slightly coarser than the dynamics grid, but more closely matches the effective resolution of the dynamics grid (W. M. Hannah et al., 2021) and reduces the grid imprinting issue reported in W. M. Hannah et al. (2020). The simulations described here also utilize the CRM variance transport scheme of W. Hannah and Pressel (2022), which remedies an unphysical checkerboard pattern identified by W. M. Hannah et al. (2022).

Ten-year (2001–2010) E3SM-MMF 2D and 3D simulations are conducted for this study with climatological input data averaged over 1995–2005, such as solar forcing, aerosol concentration, and land surface types. For the 3D configuration this is a nontrivial computational expense that has only become approachable due to the advent of GPU supercomputing and recent efforts of the US Department of Energy (DOE) Exascale Computing Project to port the MMF's CRMs to run on GPU architectures.

To investigate the role of CMT, we conduct a pair of simulations with momentum coupling activated in 2D and 3D E3SM-MMF, respectively. Note that CMT in the 2D CRM is represented using the “explicit scalar momentum transport” (ESMT) scheme of Tulich (2015), while momentum feedback in the 3D CRM is directly handled by the MMF coupling scheme similar to other prognostic fields (M. Khairoutdinov et al., 2005). We also run another 10-year simulation with E3SMv2 (non-MMF) simulation for comparison. In summary, five simulations are used in this study hereafter non-MMF, 2D, 2D with CMT (2DM), 3D, and 3D with CMT (3DM).

### 2.2. Reanalysis and Observational Datasets

To assess the performance of E3SM-MMF's precipitation events, we use the fifth generation of reanalysis (ERA5) produced by the European Center for Medium-Range Weather Forecasts (ECMWF; Hersbach et al., 2020) and the Global Precipitation Measurement Integrated Multi-satellitE Retrievals (IMERG). ERA5 provides hourly products near the surface and 37 pressure levels, with a horizontal resolution of  $0.25^\circ$ . Since reanalysis precipitation can be corrupted by the model-data fusion process intrinsic to data assimilation, we also include data from IMERG, which utilizes most of the GPM satellite constellation of passive microwave radiometers and geostationary spaceborne infrared sensors in the passive microwave-sparse regions to produce half-hourly,  $0.1^\circ \times 0.1^\circ$

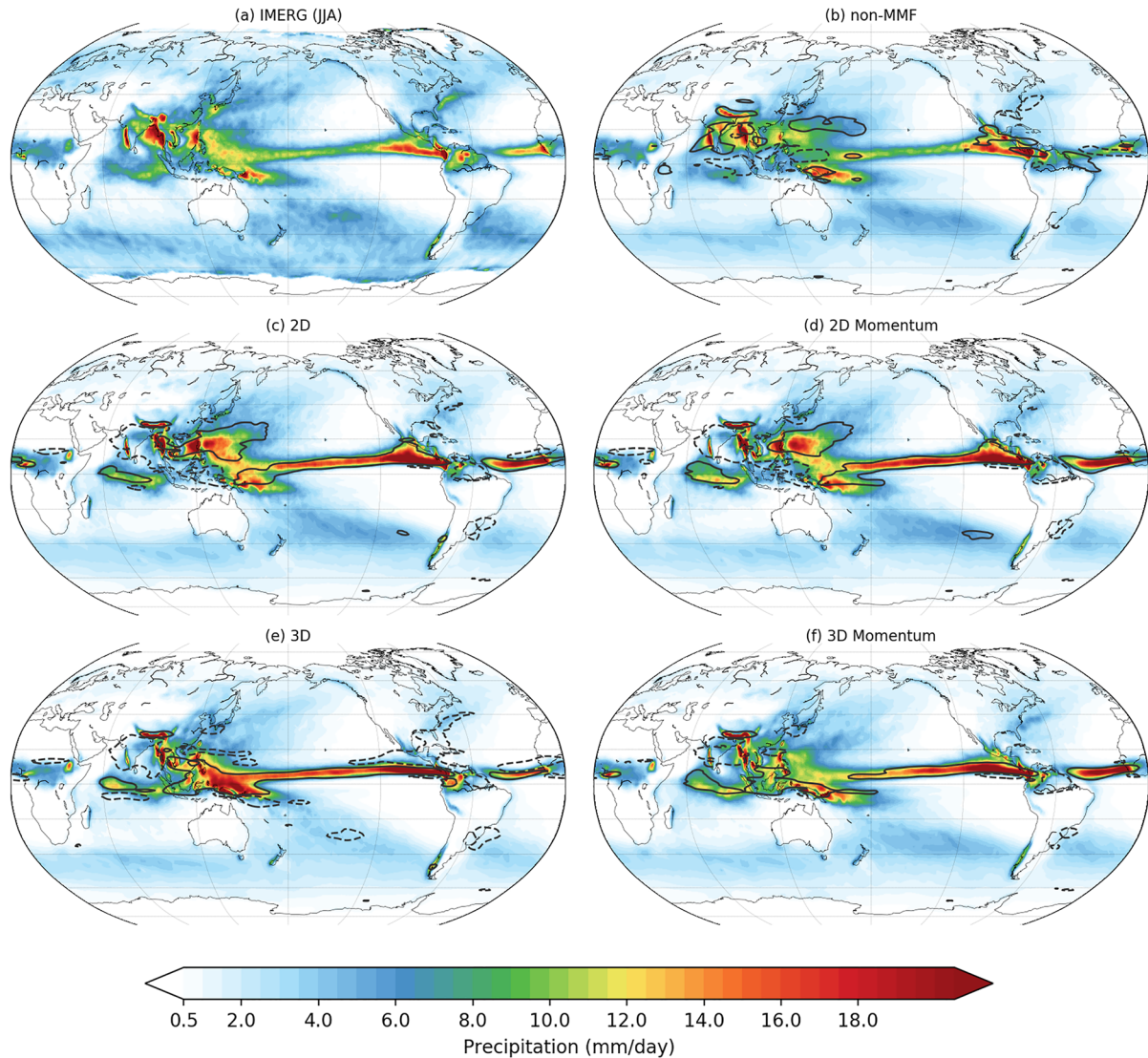


**Figure 1.** Climatological distribution of total precipitation in June–July–August (JJA), (a) IMERG, (b) non-MMF, (c) 2D, (d) 2DM, (e) 3D, (f) 3DM. The solid (dashed) lines in (b)–(f) indicate  $\pm$  2 mm/day precipitation anomaly as shown in Figure S1 in Supporting Information S1.

global precipitation products (Huffman et al., 2019). In order to compare directly with the model simulations, we regrid both the 10-year (2001–2010) ERA5 and IMERG data onto the same grid as E3SM output.

### 3. Results

#### 3.1. Climatology of Seasonal Precipitation

Figure 1 shows the mean global distribution of boreal summer (June–July–August, JJA) precipitation from observations and E3SM simulations. The solid and dashed lines in Figures 1b–1f represent large positive and negative precipitation anomalies relative to observation (Figure S1 in Supporting Information S1). To highlight the difference across MMF simulations, several strategic mean JJA precipitation difference maps are shown in Figure 2.

In general, the E3SM-MMF models share some common local problems that are not seen in non-MMF simulations, such as too intense peak time-mean rainfall in the Pacific and Atlantic Intertropical Convergence Zone (ITCZ), and not enough over the northern Amazon (Figures 1b–1f). The boreal summer wet bias in the tropical Pacific and dry bias in Amazon are also reported by Kooperman et al. (2016) using the Community Earth System Model (CESM). However, the western Pacific bias is improved with SP-CAM in Kooperman et al. (2016), while

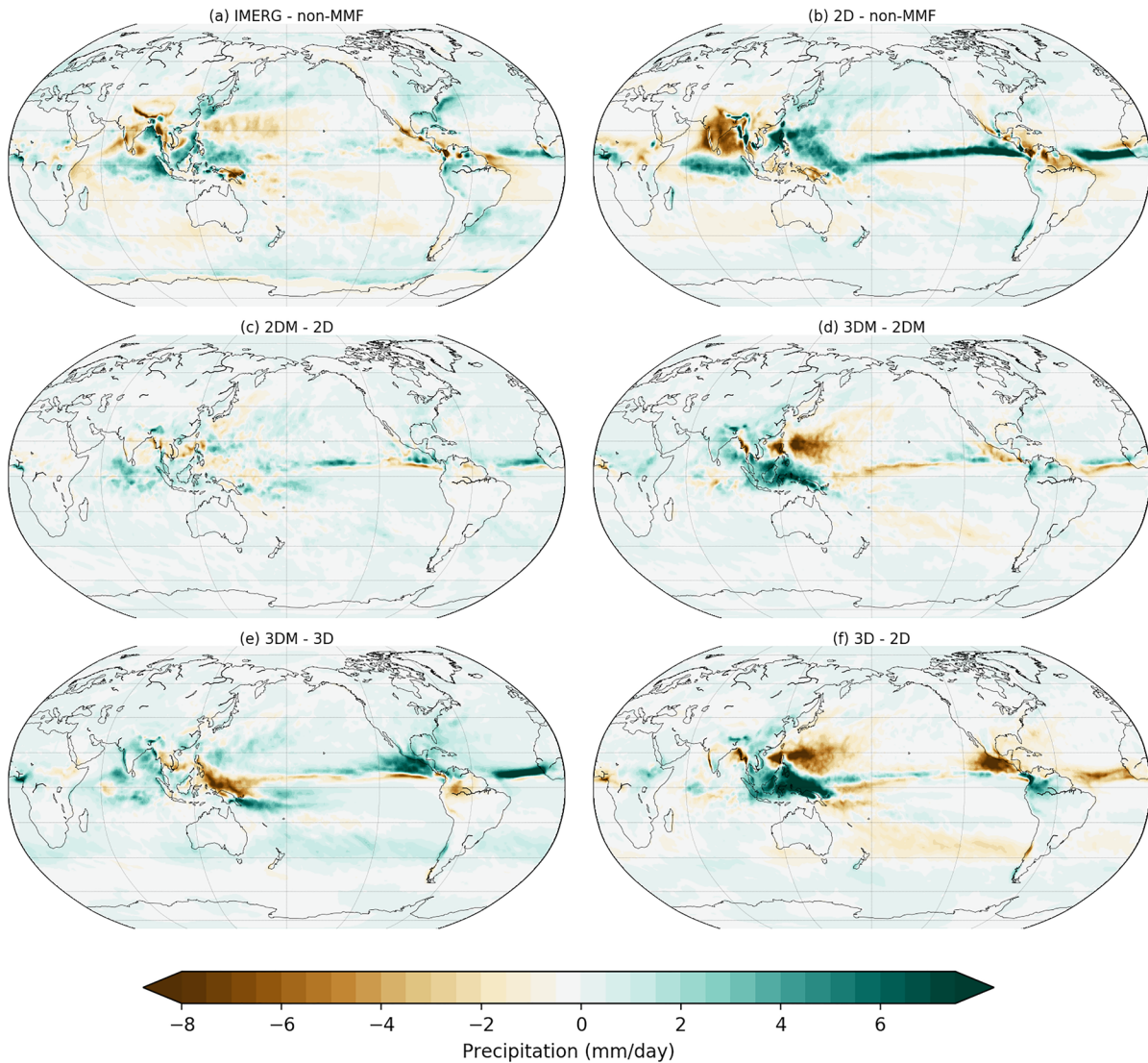


**Figure 2.** Mean JJA precipitation difference between (a) IMERG and non-MMF, (b) 2D and non-MMF, (c) 2DM and 2D, (d) 3DM and 2DM, (e) 3DM and 3D, (f) 3D and 2D.

it is only true in 3D E3SM-MMF (Figures 1e and 1f). MMF increases equatorial rainfall over the Indian Ocean and western tropical Pacific, where it is too dry in non-MMF.

Interesting sensitivities to CRM dimensionality are found in specific subregions of the tropical Pacific (Figures 2d and 2f) where a positive rainfall bias in excess of 2 mm/day occurs in both 2D MMF configurations (Figures S1b and S1c in Supporting Information S1) over the north western tropical Pacific (Figure S2 in Supporting Information S1) and eastern tropical Pacific (0°N–20°N, 120°E–150°E). This problem has been noted in many published superparameterized simulations that use prescribed sea surface temperatures (e.g., DeMott et al., 2007; M. Khairoutdinov et al., 2005; Kim et al., 2011; Luo & Stephens, 2006), for reasons that remain poorly understood. Luo and Stephens (2006) suggested that the positive rainfall bias is related to an enhanced convective-wind-evaporation feedback because of the 2D geometry of CRM. However, Kim et al. (2011) demonstrated that similar precipitation bias appears in models with conventional parameterization. Tulich et al. (2011) indicated that this significant bias is related to the overly tight coupling between convection and low-level rotation. This wet bias over the northwestern tropical Pacific is largely removed with the use of a 3D CRM domain (Figures S1d and S1e in Supporting Information S1), consistent with the result of Yang et al. (2022). They also suggested that 3D produced a weaker MJO compared to the 2D case, which can be partly attributed to the

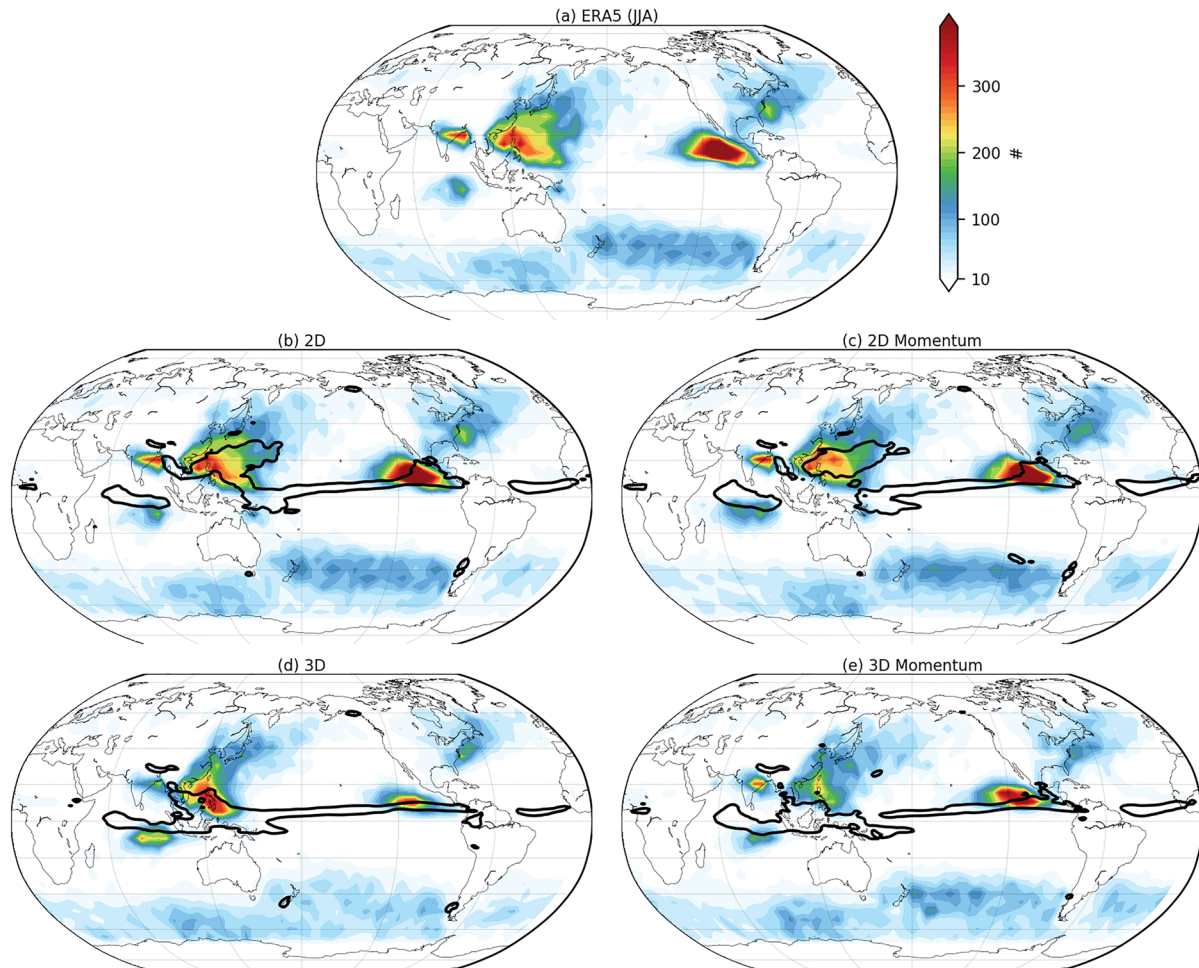


**Figure 3.** Cyclone track density from (a) ERA5, (b) 2D, (c) 2DM, (e) 3D, (f) 3DM. Black lines in panels (b)–(f) represent positive 2 mm/day precipitation anomaly compared to IMERG.

different structure of background zonal flow. Compared to the effects of CMT (Figures 2c and 2e), the dimensionality has a much larger impact on the precipitation pattern (Figures 2d and 2f).

### 3.2. Tropical Cyclone Tracking

As discussed above, dimensionality has a striking effect on the mean-state precipitation in JJA. The question naturally arises as to why, and whether a fundamental change in the characteristics of precipitating events, or their frequency, is responsible. It is well-known that tropical cyclones can account for a significant fraction of total precipitation. Therefore, it is possible that CRM dimensionality affects the characteristics of tropical cyclones. In this section, we use a Lagrangian feature-tracking approach to investigate the performance across MMF configurations, following events via their maximum relative vorticity at 850 hPa utilizing the TempestExtremes algorithm (Ullrich & Zarzycki, 2017; Ullrich et al., 2021). We use relative vorticity as an indicator of tropical cyclones because it focuses on smaller spatial scales than pressure. To capture as many of the cyclones as possible, we perform event tracking over the entire tropics and the extra-tropics. Here we only consider storms lasting for more than a day (24 hr) to eliminate the detection of short-lived cyclones.

The overall pattern of cyclone trajectories in E3SM-MMF qualitatively resembles observations (Figure S3 in Supporting Information S1), which reassures that the tracking algorithm is valid to use for model intercomparison. Track densities are shown in Figure 3 for quantitative comparison. Note that due to a non-negligible Coriolis force required to maintain the cyclonic circulation, no storm tracks are near the equator where there exists large precipitation bias across E3SM-MMF simulations. Track density is calculated by counting the number of cyclones in

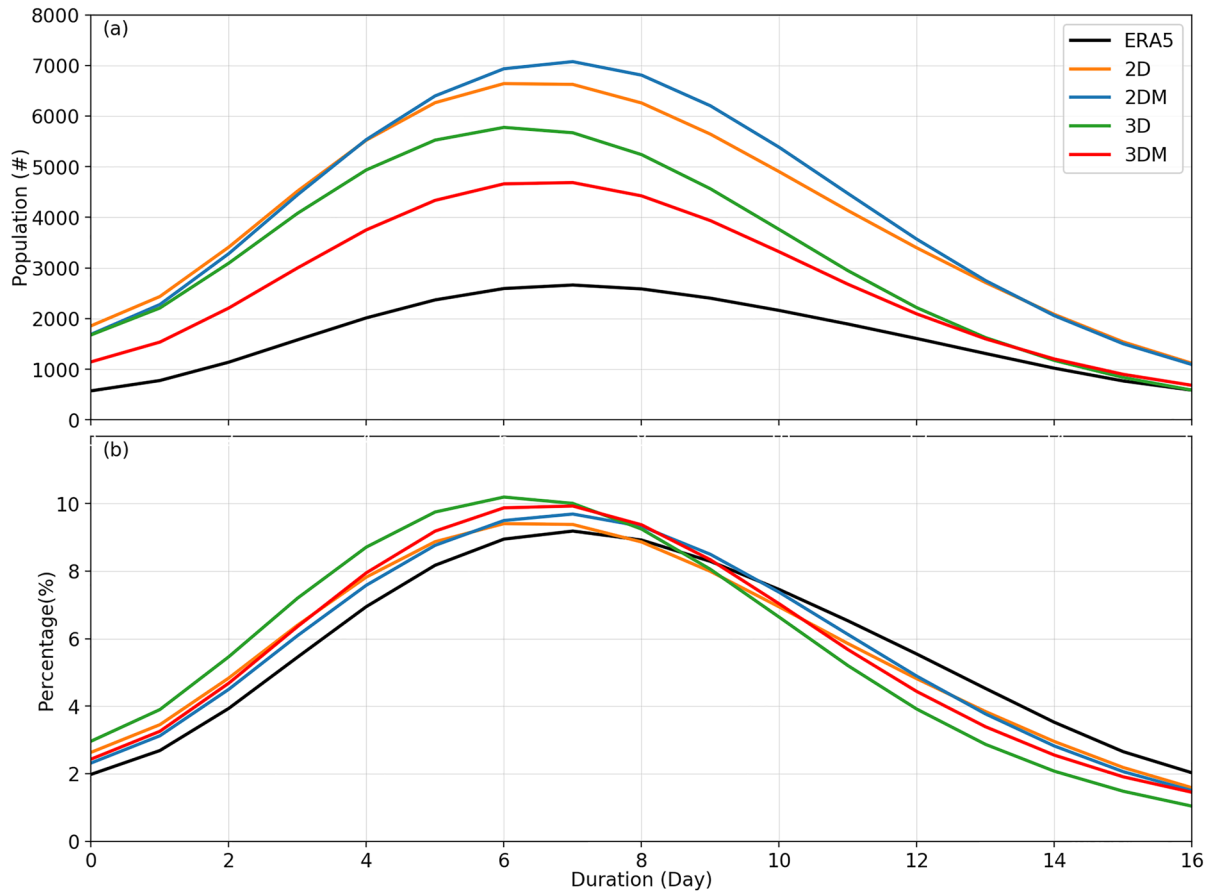


**Figure 4.** Histogram of total (a) and normalized (b) tropical cyclone durations (20°S–20°N) from ERA5 and E3SM-MMF simulations.

each  $1 \times 1^\circ$  grid point in the 3-hourly tracks for both model simulations and ERA5 reanalysis. The black contour lines represent the positive 2 mm/day precipitation anomaly compared to IMERG, which delineates the northwestern Pacific mean rainfall bias in the 2D MMF configurations (Figures 2b and 2c). Consistent with the reduction of the tropical wet bias in this region, the population of tropical cyclones in 3DE3SM-MMF has dramatically decreased. Moreover, the dramatic decrease of tracked tropical cyclones over the western Pacific is coincident with reduced precipitation bias in 3D relative to 2D (Figures S2d and S2f in Supporting Information S1).

Figure 4 shows the distribution of tracked cyclones aggregated spatially across 20°S–20°N. The number of tropical cyclones in all E3SM-MMF simulations is overestimated through all the lifetimes, compared to observations. However, this bias is reduced with both 3D and CMT, with dimensionality having a larger effect than the inclusion of CMT. This implies that a better understanding of the effect of dimensionality on precipitating event frequency may help reduce the precipitation bias in E3SM-MMF. The normalized histogram of storm durations (Figure 4b) shows that all model configurations overestimate shorter-lived storms (duration <8 days), and struggle to maintain longer-lived cyclones (duration >9 days), but that neither momentum transport nor dimensionality dramatically affect these characteristics of tracked events. Similar conclusions can be drawn from extending the analysis to the 35°S–35°N band, with different magnitudes.

Figure 5 shows the comparisons of other properties of tracked tropical cyclones, including relative vorticity at 850 hPa, precipitation rate, total column water, and relative humidity averaged over the area of  $3^\circ$  of each track storm throughout entire lifetime. Precipitation that is associated with tropical cyclones is generally overestimated (Figure 5a). The E3SM-MMF tends to produce too few weakly precipitating and too many strongly precipitating tropical cyclones, independent of its configuration. The magnitude of the precipitation bias for each precipitation rate is generally the same across all simulations. However, we note that rainfall from the heaviest precipitation events is reduced in 3D in comparison to 2D. A higher fraction of weaker vortex but a lower fraction of stronger

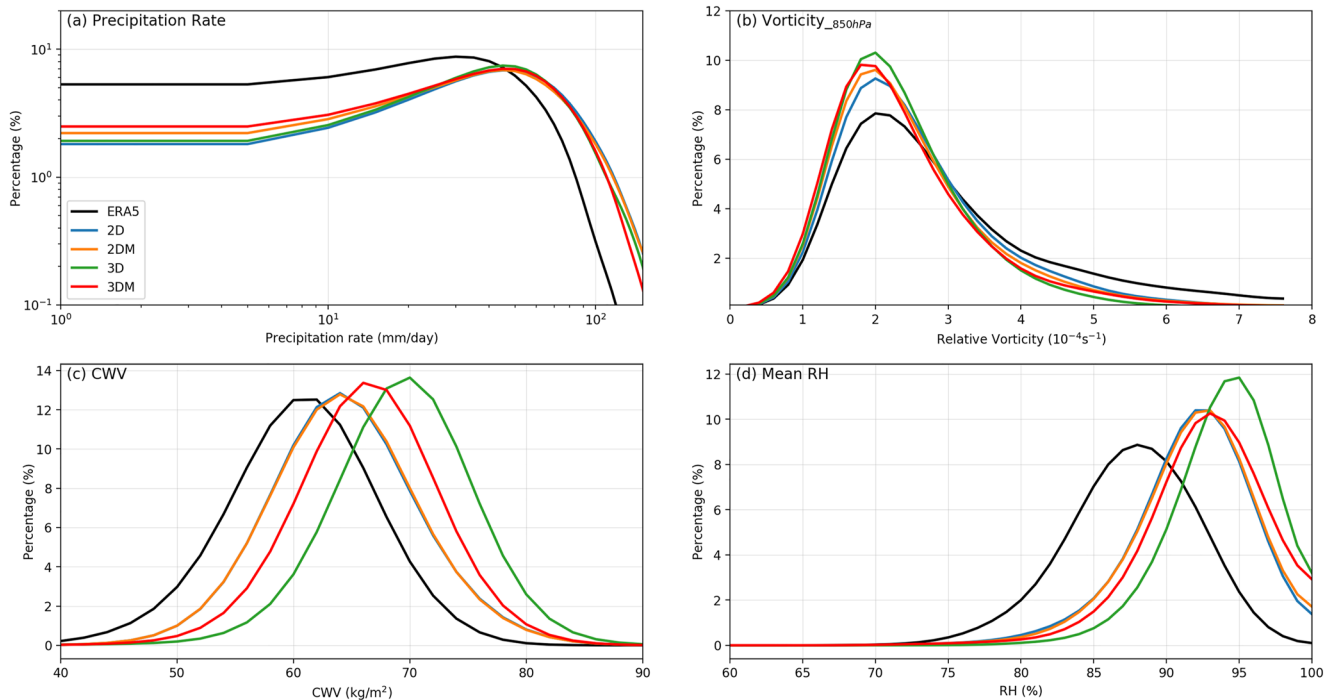


**Figure 5.** Properties of tracked tropical cyclones over tropics (20°S-20°N), (a) 3-hourly precipitation rate, (b) relative vorticity at 850 hPa, (c) column water vapor, (d) column-averaged relative humidity.

vortex in all E3SM-MMF than in ERA5 is consistent with the finding that the E3SM-MMF struggles to maintain longer-lived tropical cyclones (Figure 5b). Interestingly, the 3D simulations are characterized by higher total column water vapor (CWV) and higher relative humidity than 2D, suggesting an important change in mean state. The relationship between CWV and precipitation will be further discussed in Section 3.4.

In summary, so far our analysis of tracked vorticity events has shown that the interesting reduction in tropical northwest Pacific mean rainfall when 3D is used in place of 2D is driven, in part, by a strong reduction in the frequency of occurrence of precipitating events in this region.

### 3.3. Dilution Hypothesis

The above analysis makes it clear that dimensionality has a striking effect on the mean state precipitation but has not resolved why. The differences in the CWV for tracked tropical cyclones offer a first clue. We suspect a dependence of the way cloudy and clear sky air mix with each other on CRM dimensionality. Petch et al. (2008) suggested that in the lower-troposphere, updrafts in 3D CRMs “mix” with the environment significantly more than updrafts in 2D CRMs, with updrafts in 3D CRMs both entraining and detraining larger fractions of their mass than in 2D. This matters given that dilution by entrainment of dry environmental air reduces updraft buoyancy, which can limit the development of convection in relatively dry columns. According to Petch et al. (2008), a plume in three dimensions experiences larger fractional mixing than a plume of the same width in two dimensions because it has a greater surface area than a plume of the same width in two dimensions, and this leads to larger dilution by entrainment. This argument assumes that localized interfacial mixing and mass exchange is the same between 2D and 3D clouds, which may or may not be true. Additionally, numerous studies have also indicated that 2D updrafts tend to be weaker than 3D updrafts (e.g., Morrison, 2016; Murray et al., 1970; Zeng et al., 2008). Morrison (2016) attributed the weakness of 2D updraft to perturbation pressure forces due to difference in mass continuity between 2D and 3D. Stronger 3D updraft result in higher vertical velocity gradients, leading to more fractional entrainment and detrainment, as well as more evaporation of cloud water and lower precipitation efficiency (PE). From this view, higher free-tropospheric humidity might be required to produce the same surface precipitation rate in a 3D CRM.

In the following section we will present evidence that suggests (although does not directly prove) that updrafts in the 3D MMF configurations exchange more mass with the environment than updrafts in 2D: A moisture-precipitation

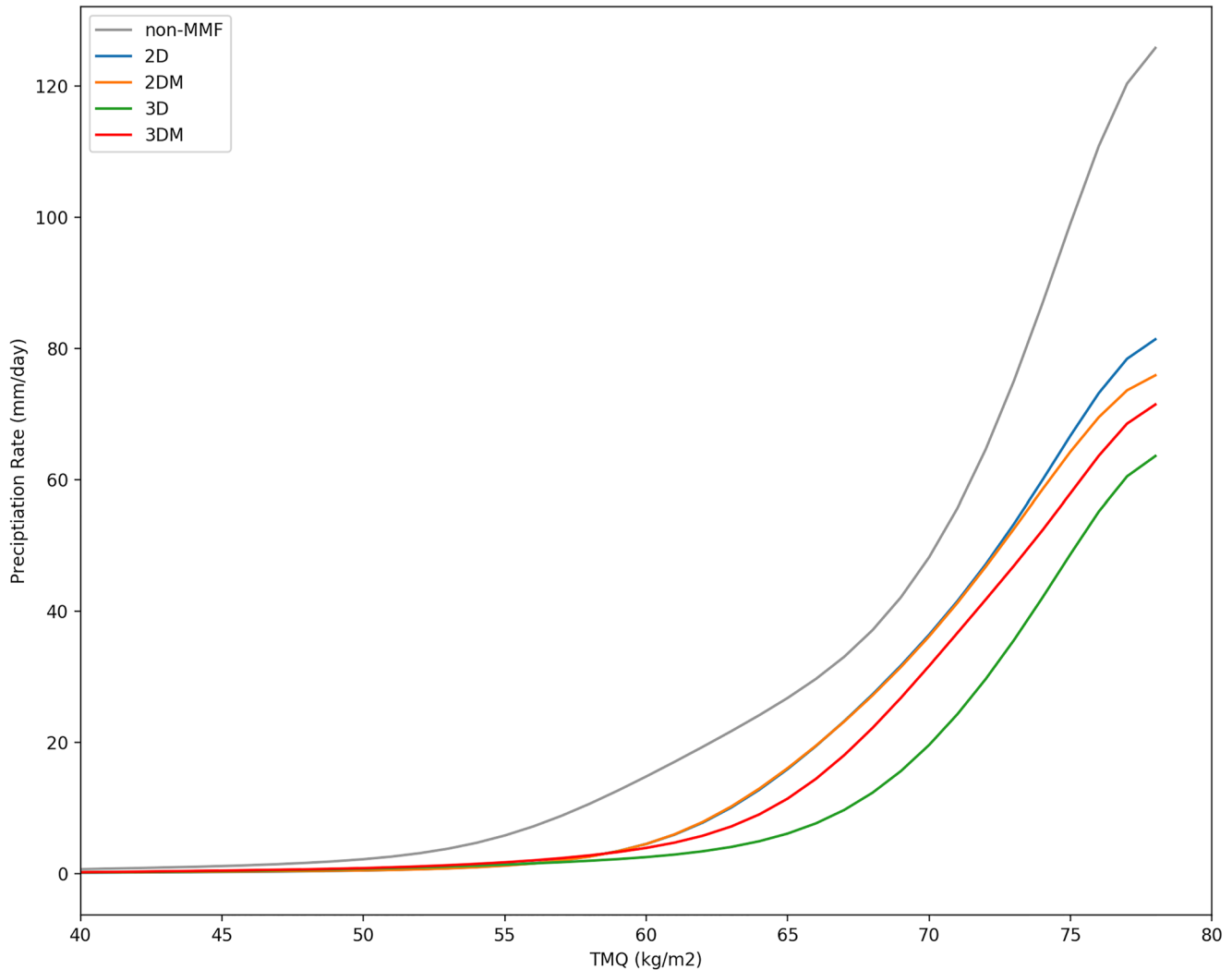


**Figure 6.** Relationship between 3-hourly precipitation rate and total precipitation water over tropical western Pacific.

pickup that is associated with a higher vapor path, a smaller PE, and amplified convective mass flux profiles and high cloud fraction.

### 3.4. Evidence Supporting a Dimensionality-Dilution Framework

#### 3.4.1. 3D Shifts Precipitation Onset to a Higher Water Vapor Path

A well-known relationship between the CWV and precipitation has been identified by many studies (e.g., Bretherton et al., 2004; Muller et al., 2009; Peters & Neelin, 2006; B. O. Wolding, Dias, Kiladis, Ahmed, et al., 2020; B. Wolding, Dias, Kiladis, Maloney, & Branson, 2020), and dilution by entrainment processes has been revealed to be instrumental in explaining this relationship due to the differences in buoyancy between diluted and moist air (Kuo et al., 2017).

Figure 6 shows the precipitation rate as a function of total vertically integrated precipitable water, or CWV based on 3-hourly output from 10-year simulations. The critical CWV threshold (henceforth, “pickup”), at which there is a rapid increase of precipitation with CWV, occurs at different values in each simulation. The non-MMF exhibits a much earlier pickup than all the E3SM-MMF configurations.

The main point to take from Figure 6 is that the precipitation pickup is shifted to higher vapor in the E3SM-MMF simulations with 3D CRMs compared to 2D. This could be viewed as consistent with our suspicion that there is

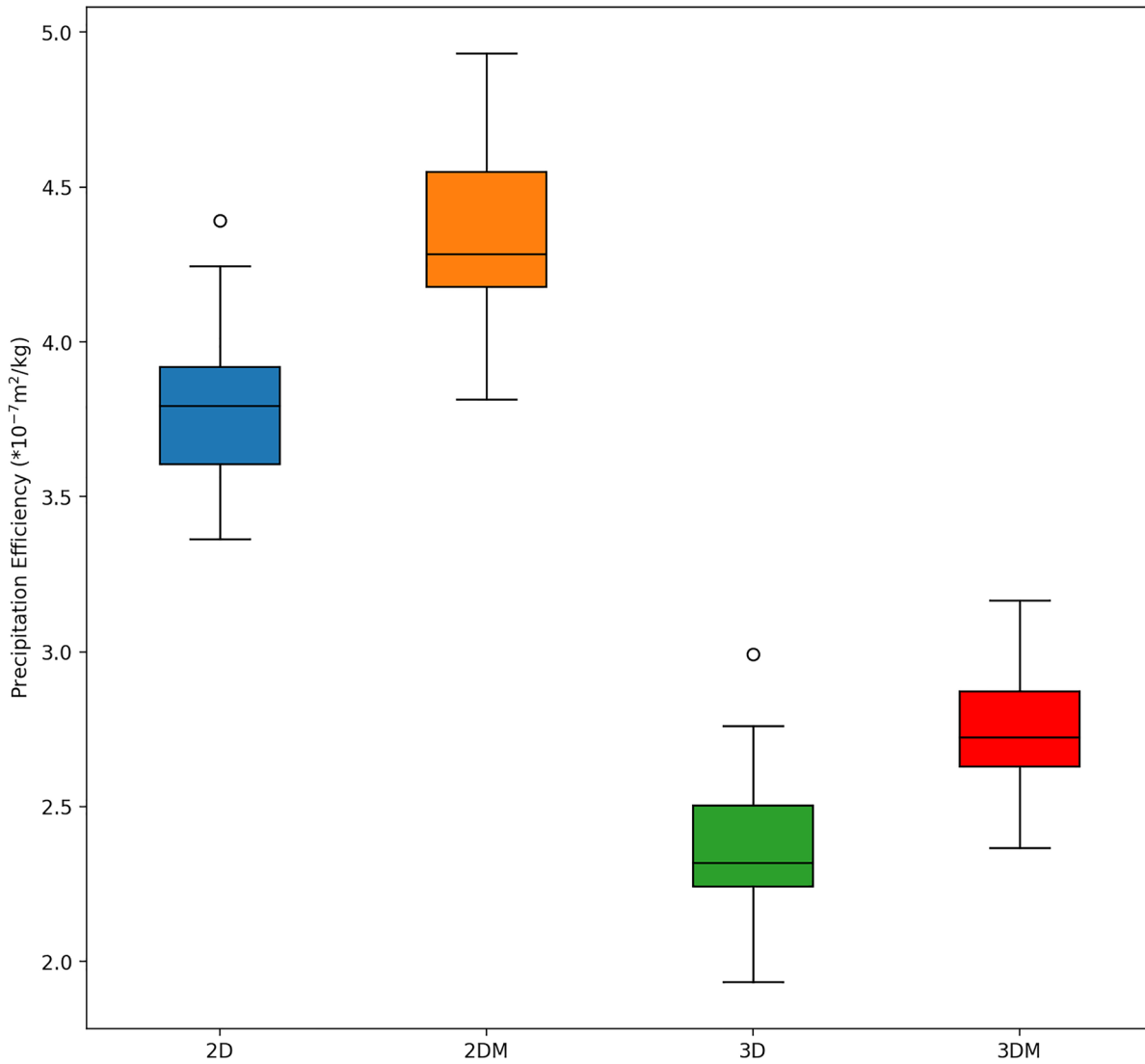


**Figure 7.** Boxplot of precipitation efficiency across E3SM-MMF configurations. Lines at each box represent (from bottom to top) the minimum, the 25th, 50th (median), 75th, and the maximum values.

weaker dilution by entrainment in 2D since convection that mixes less with its environment is less limited in its ability to produce precipitation by a drier free troposphere.

### 3.4.2. 3D Reduces Precipitation Efficiency

A corollary of the idea that more water vapor is required for the same amount of precipitation under a condition with more mixing is that PE is expected to be lower to overcome the stronger dilution barrier in 3D. Wilson and Toumi (2005) proposed that accumulated precipitation can be described as a product of three factors:  $R_{acc} = \kappa m$ , where  $m$  is the mass of air advected into the column and pushed through the moist level, and  $\kappa$  is the instantaneous PE. We posit that precipitation can be expressed as proportional to three variables: mass flux, specific humidity, and PE. Hence, we define PE here as

$$PE = \frac{P}{\int_{1,000\text{hPa}}^{5\text{hPa}} mq} \quad (1)$$

where  $q$  is the specific humidity,  $P$  is the precipitation rate, and  $m$  is the vertically integrated updraft mass flux from CRM. With this definition, we can consider PE as precipitation per unit of moisture convergence. Figure 7 displays

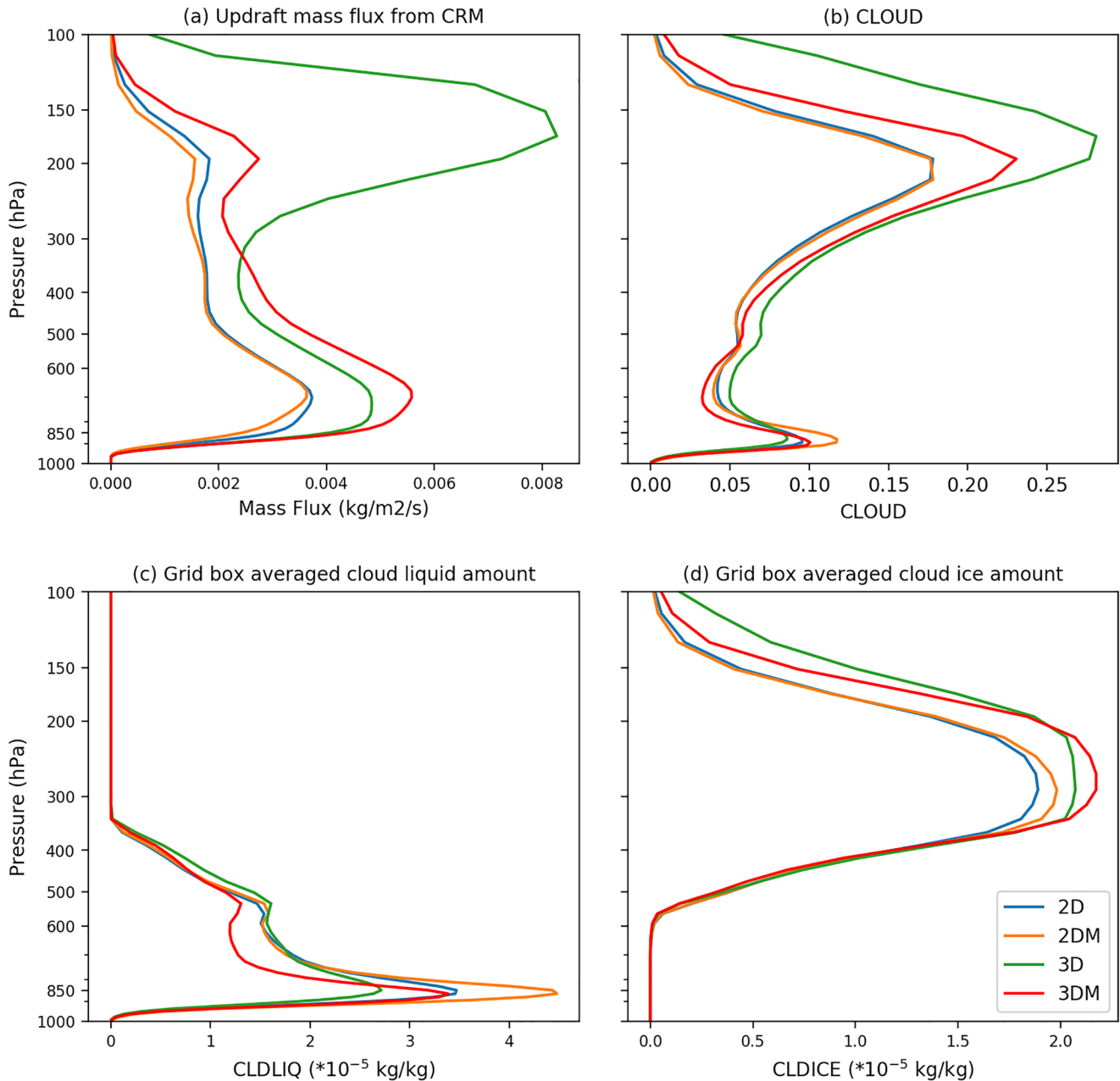


**Figure 8.** Profiles of (a) updraft mass flux, (b) cloud fraction, (c) cloud liquid amount, (d) cloud ice amount across E3SM-MMF configurations. The profiles are derived from tropics (20°S-20°N).

the box plot of PE values based on monthly output from 10-year E3SM-MMF simulations. Lines at each box represent (from bottom to top) the minimum, the 25th, 50th (median), 75th, and the maximum values. The open circles indicate the outliers. Consistent with our expectation, PE is lower in 3D, meaning that 2D precipitation is greater than 3D for a given mass advection from the surrounding regions, in agreement with the stronger dilution hypothesis in 3D. Although dimensionality has a larger effect on this statistic than CMT, it is interesting to note the secondary sensitivity that E3SM-MMF with CMT in both 2D and 3D simulations have a higher PE than without momentum coupling.

### 3.4.3. 3D Amplifies Convective Mass Flux Profiles and High Cloud Amounts

Another line of evidence of increased entrainment and detrainment in 3D can be found in the statistics of the updraft mass flux by using 10-year monthly outputs (Figure 8a). The updraft mass flux is obtained by multiplying the updraft speed greater than 2 m/s with air density when non-precipitating cloud water and ice content is greater

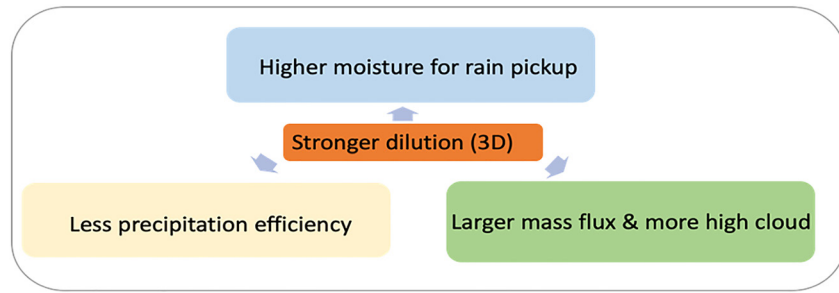


**Figure 9.** Diagram of a dilute framework with multiple indirect lines of supportive evidence.

than 1 g/kg. The larger low-level (around 700 hPa) peak in updraft mass flux in 3DM indicates more sub-cloud entrainment than in 2DM. Additionally, the difference between the low-level peak in updraft mass flux and the mid-tropospheric minimum around 400 hPa is larger in 3DM than in 2DM, indicating more detrainment in those simulations. This occurs despite a reduced boundary layer cloud liquid amount (Figure 8c). As an aside, we note that the 3D simulation without momentum transport was an outlier having an inexplicable symptom of substantially larger top-heavy convection and high cloudiness, for reasons we have not attempted to explain, and thus we have focused this part of the analysis on the better-behaved simulation pair that included momentum coupling.

Jeevanjee and Zhou (2022) demonstrated that cloud resolving simulations with stronger mixing tend to also produce more high clouds, and this is also consistent with our simulations. Both 3D configurations of the MMF produce systematically higher cloud fraction and ice concentrations above 400 hPa (Figures 8b and 8d). It is also interesting to note that something unusual occurred leading to extremely top-heavy convection and anomalously large high cloud fractions in just the 3D simulation that did not use CMT. It is interesting, but beyond the scope of this paper to investigate, that CMT modulated the high cloud amount so strongly in the 3D configuration, while having minimal impact in the 2D configuration.

Even though we cannot directly measure or assess dilution by entrainment in the current version of E3SM-MMF, multiple indirect lines of evidence have pointed to a change in it with dimensionality. As sketched in Figure 9, 3D updrafts exchange more mass with the environment than 2D updrafts, leading to a stronger dilution by entrainment and more water vapor required for convection to occur. Meanwhile, stronger dilution in 3D can result in more evaporation and a lower PE, leading to larger mass flux and more high clouds.

### 3.5. Fast-Time Scale Effects During Initialization and a Connection to Extremes

We have provided quantitative support of the mechanism proposed in Figure 9, namely that stronger dilution by entrainment in 3D leads to a higher rain pickup, a smaller PE, an increased updraft mass flux, and more anvil clouds. We now turn to a practical question as to whether these consequences of dimensionality could have been anticipated in just the first few days of sensitivity tests.

Figure 10 shows comparison of the total grid-box liquid water path (boxplots summarize the geographic distribution of temporal snapshots) and the 99th percentile of vertical velocity at 500 hPa during the initialization of each simulation across MMF configurations. During the first day of the simulation, 2D produces more liquid water path than 3D (Figure 10a), suggesting the fast response of dimensionality impact. We interpret the enhanced liquid in the 2D configuration as the signal of a system that is struggling less against mixing with its environment to maintain low level liquid water clouds. Moreover, the notable initial difference in the liquid path between 2D and 3D persists after 1 month (Figure 10b). This implies that the long-term climatology of precipitating events can be predicted by these fast-time scale effects, providing an opportunity for rapid model tuning and optimization using short integrations without the high computational cost.

Figure 10 also reveals an interesting response of extreme statistics to rainfall. Like the liquid cloud response, this geographic extreme signal is immediately detectable within the first simulated day, with the difference persisting over the subsequent month. Stronger extreme updrafts in 2D are consistent with the stronger tails of extreme precipitation that we noted in Figure 5a. This is not immediately easy to reconcile as a consequence of entrainment and we do not attempt to explain the causal origins of the extreme response, other than to emphasize that two important aspects of a global cloud resolving simulation worth calibrating—time mean rainfall and extreme

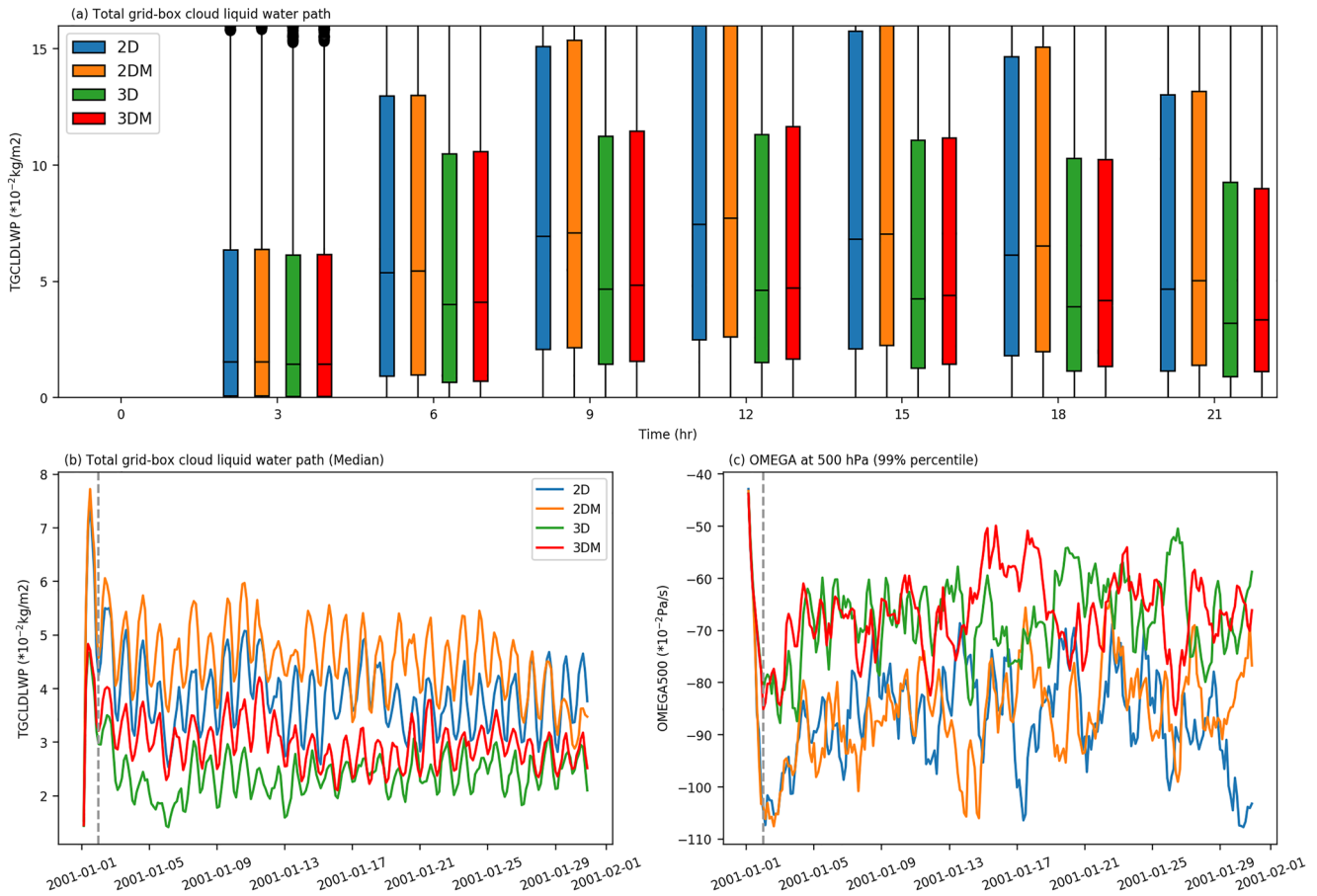


**Figure 10.** Comparison of liquid water path and omega at 500 hPa during initialization across E3SM-MMF configurations: (a) boxplot of total cloud liquid water path during the first day of initialization, (b) median of total cloud liquid water path for the first month of simulations, (c) 99% percentile updraft (omega) at 500 hPa. The gray dashed vertical lines in (b) and (c) indicate the end of the first day of the simulation, during which the initial adjustments in (a) occurred.

statistics—may both be controllable through the domain dimensionality of an MMF and might be possible to think about through a unified entrainment framework.

#### 4. Concluding Discussion

In this study, we examined the representation of precipitation from a set of modern E3SM-MMF simulations that use different dimensionality and momentum transport, namely non-MMF, 2D, 2D with CMT, 3D, and 3D with CMT. Compared to previous MMF generations for whom computational limitations prohibited testing the effects of using ambitious 3D domains, the GPU-accelerated E3SM-MMF has penetrated new frontiers.

Compared to non-MMF, the E3SM-MMF produces too intense rainfall in ITCZ, and not enough rainfall over the northern Amazon. However, robust improvements due to MMF include increased on-equatorial rainfall over the Indian Ocean and western tropical Pacific, where it is too dry in non-MMF. Most interestingly, the results reveal some distinct differences in the mean-state precipitation pattern over subregions of the tropics across the multiple MMF configurations. For instance, the 2D MMF produces an unrealistically rainy region over the northwestern and eastern tropical Pacific, while these regional biases are significantly reduced when a 3D CRM is used in E3SM-MMF. With both the effect of dimensionality and CMT, 3D with a CMT configuration shows a significant improvement of precipitation relative to 2D without a CMT. The difference in precipitation between 2D and 3D is consistent with the findings of Yang et al. (2022), who also suggested that 3D produced a weaker MJO than 2D, partly due to difference in the zonal flow. However, in comparison to the striking effect of dimensionality, impacts of CMT are minor in reducing this precipitation bias. Trajectory analysis indicates that these regional improvements of time-mean precipitation simulation in the northwestern and eastern tropical Pacific

are associated with fewer tropical cyclones in 3D E3SM-MMF. The composite analysis of tropical cyclones showed that the low-level vorticity is slightly weaker in 3D than that in 2D (Figure S5 in Supporting Information S1), consistent with the findings of Tulich et al. (2011), who attributed the precipitation bias to the overly tight coupling between convection and vorticity. However, our analysis also revealed that the correlation between convection and vorticity over the tropical northern hemisphere (0°N–20°N) is not significantly different compared to ERA5 (Figure S6 in Supporting Information S1). This highlights the need to further explore and understand the causes of this precipitation bias.

In attempting to understand why and how the representation of precipitation is improved in 3D E3SM-MMF, we have proposed a framework—that dilution by entrainment is stronger in 3D relative to 2D. Conceptually, this is rooted in two simple geometric ideas: an updraft in 3D has more surface area to mix with the environment than an updraft of the same width in 2D, and a stronger updraft in 3D than in 2D as a result of difference in mass continuity. Empirically, it can be connected to multiple sensitivities we observed across our experiments. Stronger dilution of dry air reduces updraft buoyancy and suppresses convection until the lower troposphere is sufficiently moistened, meaning more water vapor is required for rain pickup; delayed rainfall pickup is seen in our 3D MMF configurations (Figure 6). Rotunno and Emanuel (1987) suggested that the nature of cyclogenesis is due to boundary layer divergence caused by downdraft and a weak disturbance can amplify only when the middle level is moist enough to suppress downdraft and increase PE. Stronger entrainment, however, decreases PE and slows the spin-up of the low-level circulation (Raymond et al., 2007). This is because the upward convective mass flux is decreased by the high entropy deficit created by convective downdraft and the entrainment of low-entropy air into the boundary layer (Emanuel, 1995; Tang et al., 2016; Thayer-Calder & Randall, 2015). This also reduces the buoyancy of the updrafts, leading to a less efficient spin-up of the low-level circulation and a longer time for the deep tropospheric moisture to increase (James & Markowski, 2010; Smith & Montgomery, 2012), consistent with less cloud liquid water in 3D than in 2D during the initialization (Figure 10).

We demonstrate that precursor signals suggestive of the significant difference in the mean state precipitation and extreme tail behavior across E3SM-MMF configurations can be identified even in the first few simulated days of output. This may provide an opportunity for rapid model tuning to improve precipitation representation in the climate model and advance the understanding of mechanisms driving precipitation events. This can be achieved by investigating cloud feedback dynamics through the tuning of the interior physics before launching multidecadal simulations. For example, Peng et al. (2023) partially resolved the over-entrainment issue of low clouds in current MMFs by using hyperviscosity and cloud droplet sedimentation, providing opportunity to study low cloud feedback dynamics with reduced parameterization.

The findings of this study raise a number of questions and potential future research topics. Wet-ITCZ and dry-Amazon biases appear to be a recurring bias in the current generation of E3SM-MMF; it will be interesting to discover whether ocean coupling impacts these signals, or whether tuning strategies can address them. An obvious limitation of our analysis is that no direct observations of entrainment or dilution exist for quantitative confirmation. Rather, the proposed dilution framework is supported by mechanisms that are associated with the dilution by entrainment as displayed in the summary diagram (Figure 9). Nevertheless, our results are generally consistent with other studies (Jeevanjee & Zhou, 2022; Petch et al., 2008; Phillips & Donner, 2006; Tompkins & Semie, 2017). For example, Tompkins and Semie (2017) explored the role of entrainment in convection organization. They argued that the strength of updraft dilution by entrainment controls the onset of convective organization. With cloud-resolving simulations, Jeevanjee and Zhou (2022) indicate that an increase in cloud fraction with horizontal resolution can be traced back to enhanced horizontal mixing, which increases evaporation of condensed water and decreases PE, consequently resulting in an increased mass flux and more high cloud. The consistency of our results with previous studies using different models imply that the findings of this study are not model dependent.

Another considerable caveat of this work is that the impact of CMT remains unclear, and we have not focused on it, despite some interesting evidence of impact especially in 3D. Several results of this study suggest that the influence of CMT on the mean-state precipitation and extreme precipitation is not as significant as the dimensionality. However, momentum coupling implicates some intriguingly strong sensitivities of the 3D E3SM-MMF. Without CMT, 3D MMF tends to exhibit a much later rain pick-up, a large increase in high cloud amount and associated convective mass flux, and lower values of PE. This highlights the importance of CMT in the more accurate representation of precipitating events in climate models. We note that the 3D E3SM-MMF that includes CMT compared best against rainfall observations in our initial analysis.

The notable difference between 2D and 3D during the initialization implies that the first week or month of simulation can be treated as a forecast for longer-term behavior. Initial signals like low cloud liquid content and extreme storm development may be helpful precursors for tuning longer term regional rainfall anomalies, and could be viewed as consistent through a dilution framework. If confirmed, this could provide an additional constraint in quick model validation and comparison across different configurations. The 3D MMF configurations explored in this study were not trivial to compute, but made possible by GPU supercomputing. With global storm resolving simulations remaining expensive yet increasing in popularity, precursor signals that can be linked to climatological calibration targets of mean rainfall and extreme skill are of high interest today.

Finally, a preliminary investigation of convection size during the first month of model initiation suggested that convection can develop into more organized convection in 3D. As shown in Figure S4 in Supporting Information S1, precipitation events tend to be larger in 3D than in 2D, with the mean volumetric rain (a product of precipitation area and the mean rain rate) smaller. Given the importance of precipitation to global and regional water and energy balances, further exploration of how dimensionality and momentum affect convection organization seems warranted.

### Data Availability Statement

The E3SM-Multi-scale Modeling Framework (E3SM-MMF) source code is available on the GitHub repository (<https://github.com/E3SM-Project/E3SM>). The branch for this study can be archived at W. Hannah et al. (2022) (<https://doi.org/10.5281/zenodo.6561445>). The ERA5 data can be obtained from <https://www.ecmwf.int/en/forecasts/datasets/reanalysis-datasets/era5>. The IMERG precipitation products can be downloaded from Goddard Earth Sciences Data and Information Services Center (GES DISC) (<https://disc.gsfc.nasa.gov/>).

### Acknowledgments

We would like to thank Stefan Tulich and another anonymous reviewer for extremely helpful feedback on the manuscript. This research was supported by the Exascale Computing Project (17-SC-20-SC), a collaborative effort of the U.S. Department of Energy Office of Science and the National Nuclear Security Administration, and the Energy Exascale Earth System Model (E3SM) project, funded by the Department of Energy office and the office of Biological and Environmental Research. The authors thank the Department of Energy Office of Science for funding under Grant DE-SC0023368. This research has been supported by the National Oceanic and Atmospheric Administration Climate & Global Postdoctoral Fellowship Program through UCAR CPAESS Grant NA18NWS4620043B. This work was performed under the auspices of the U.S. Department of Energy by Lawrence Livermore National Laboratory under Contract DE-AC52-07NA27344. The analysis of this study is performed using computational resources provided by the National Energy Research Scientific Computing Center (NERSC), a DOE Office of Science User Facility supported by the Office of Science of the U.S. The authors also thank the Texas Advanced Computing Center (TACC) at The University of Texas at Austin (<http://www.tacc.utexas.edu>) for their support. Additionally, the authors appreciate the resources provided by the XSEDE's PSC Bridges-2 system, which is funded by the National Science Foundation Grants ACI-1548562 and ACI-1928147.

### References

- Allen, M. R., & Ingram, W. J. (2002). Constraints on future changes in climate and the hydrological cycle. *Nature*, *419*(6903), 224–232. <https://doi.org/10.1038/nature01092>
- Benedict, J. J., & Randall, D. A. (2009). Structure of the Madden-Julian oscillation in the superparameterized CAM. *Journal of the Atmospheric Sciences*, *66*(11), 3277–3296. <https://doi.org/10.1175/2009jas3030.1>
- Bogenschutz, P. A., Gettelman, A., Morrison, H., Larson, V. E., Craig, C., & Schanen, D. P. (2013). Higher-order turbulence closure and its impact on climate simulations in the community atmosphere model. *Journal of Climate*, *26*(23), 9655–9676. <https://doi.org/10.1175/JCLI-D-13-00075.1>
- Bretherton, C. S., Peters, M. E., & Back, L. E. (2004). Relationships between water vapor path and precipitation over the tropical oceans. *Journal of Climate*, *17*(7), 1517–1528. [https://doi.org/10.1175/1520-0442\(2004\)017<1517:rbwvpa>2.0.co;2](https://doi.org/10.1175/1520-0442(2004)017<1517:rbwvpa>2.0.co;2)
- Dai, A. (2006). Precipitation characteristics in eighteen coupled climate models. *Journal of Climate*, *19*(18), 4605–4630. <https://doi.org/10.1175/JCLI3884.1>
- Dai, A., & Trenberth, K. E. (2004). The diurnal cycle and its depiction in the community climate system model. *Journal of Climate*, *17*(5), 930–951. [https://doi.org/10.1175/1520-0442\(2004\)017<0930:TDCAID>2.0.CO;2](https://doi.org/10.1175/1520-0442(2004)017<0930:TDCAID>2.0.CO;2)
- Dai, A., Trenberth, K. E., & Karl, T. R. (1999). Effects of clouds, soil moisture, precipitation, and water vapor on diurnal temperature range. *Journal of Climate*, *12*(8), 2451–2473. [https://doi.org/10.1175/1520-0442\(1999\)012<2451:eocsmv>2.0.co;2](https://doi.org/10.1175/1520-0442(1999)012<2451:eocsmv>2.0.co;2)
- DeMott, C. A., Randall, D. A., & Khairoutdinov, M. (2007). Convective precipitation variability as a tool for general circulation model analysis. *Journal of Climate*, *20*(1), 91–112. <https://doi.org/10.1175/JCLI3991.1>
- Deng, L., & Wu, X. (2010). Effects of convective processes on GCM simulations of the Madden-Julian oscillation. *Journal of Climate*, *23*(2), 352–377. <https://doi.org/10.1175/2009jcli3114.1>
- Donat, M. G., Lowry, A. L., Alexander, L. V., O’Gorman, P. A., & Maher, N. (2016). More extreme precipitation in the world’s dry and wet regions. *Nature Climate Change*, *6*(5), 508–513. <https://doi.org/10.1038/nclimate2941>
- Emanuel, K. A. (1995). The behavior of a simple hurricane model using a convective scheme based on subcloud-layer entropy equilibrium. *Journal of the Atmospheric Sciences*, *52*(22), 3960–3968. [https://doi.org/10.1175/1520-0469\(1995\)052<3960:tboash>2.0.co;2](https://doi.org/10.1175/1520-0469(1995)052<3960:tboash>2.0.co;2)
- Gettelman, A., Morrison, H., Santos, S., Bogenschutz, P., & Caldwell, P. M. (2015). Advanced two-moment bulk microphysics for global models. Part II: Global model solutions and aerosol–cloud interactions. *Journal of Climate*, *28*(3), 1288–1307. <https://doi.org/10.1175/JCLI-D-14-00103.1>
- Golaz, J., Larson, V. E., & Cotton, W. R. (2002). A PDF-based model for boundary layer clouds. Part I: Method and model description. *Journal of the Atmospheric Sciences*, *59*(24), 3540–3551. [https://doi.org/10.1175/1520-0469\(2002\)059<3540:APBMFB>2.0.CO;2](https://doi.org/10.1175/1520-0469(2002)059<3540:APBMFB>2.0.CO;2)
- Grabowski, W. W. (2001). Coupling cloud processes with the large-scale dynamics using the cloud-resolving convection parameterization (CRCP). *Journal of the Atmospheric Sciences*, *58*(9), 978–997. [https://doi.org/10.1175/1520-0469\(2001\)058<0978:CCPWTL>2.0.CO;2](https://doi.org/10.1175/1520-0469(2001)058<0978:CCPWTL>2.0.CO;2)
- Grabowski, W. W., & Smolarkiewicz, P. K. (1999). CRCP: A cloud resolving convection parameterization for modeling the tropical convecting atmosphere. *Physica D*, *133*(1–4), 171–178. [https://doi.org/10.1016/s0167-2789\(99\)00104-9](https://doi.org/10.1016/s0167-2789(99)00104-9)
- Hannah, W., & Pressel, K. (2022). Transporting CRM variance in a multiscale modelling framework. *EGUsphere*. <https://doi.org/10.5194/egusphere-2022-397>
- Hannah, W., Pressel, K., Ovchinnikov, M., & Elsaesser, G. (2022). Checkerboard patterns in E3SMv2 and E3SM-MMFv2. *Geoscientific Model Development*, *15*, 6243–6257. <https://doi.org/10.5194/gmd-15-6243-2022>
- Hannah, W. M., Bradley, A. M., Guba, O., Tang, Q., Golaz, J.-C., & Wolfe, J. (2021). Separating physics and dynamics grids for improved computational efficiency in spectral element earth system models. *Journal of Advances in Modeling Earth Systems*, *13*(7), e2020MS002. <https://doi.org/10.1029/2020MS002419>

- Hannah, W. M., Jones, C. R., Hillman, B. R., Norman, M. R., Bader, D. C., Taylor, M. A., et al. (2020). Initial results from the super-parameterized E3SM. *Journal of Advances in Modeling Earth Systems*, *12*(1), e2019MS001863. <https://doi.org/10.1029/2019MS001863>
- Hersbach, H., Bell, B., Berrisford, P., Hirahara, S., Horanyi, A., Munoz-Sabater, J., et al. (2020). The ERA5 global reanalysis. *Quarterly Journal of the Royal Meteorological Society*, *146*(730), 1999–2049. <https://doi.org/10.1002/qj.3803>
- Houze, R. A. (2004). Mesoscale convective systems. *Reviews of Geophysics*, *42*(4), RG4003. <https://doi.org/10.1029/2004RG000150>
- Huang, D.-Q., Yan, P., Zhu, J., Zhang, Y., Kuang, X., & Cheng, J. (2017). Uncertainty of global summer precipitation in the CMIP5 models: A comparison between high-resolution and low-resolution models. *Theoretical and Applied Climatology*, *132*(1–2), 55–69. <https://doi.org/10.1007/s00704-017-2078-9>
- Huffman, G. J., Stocker, E. F., Bolvin, D. T., Nelkin, E. J., & Tan, J. (2019). *GPM IMERG final precipitation L3 half hourly 0.1 degree x 0.1 degree V06*. Goddard Earth Sciences Data and Information Services Center (GES DISC). <https://doi.org/10.5067/GPM/IMERG/3B-HH/06>
- James, R. P., & Markowski, P. M. (2010). A numerical investigation of the effects of dry air aloft on deep convection. *Monthly Weather Review*, *138*(1), 140–161. <https://doi.org/10.1175/2009mwr3018.1>
- Jeevanjee, N., & Zhou, L. (2022). On the resolution-dependence of anvil cloud fraction and precipitation efficiency in radiative-convective equilibrium. *Journal of Advances in Modeling Earth Systems*, *14*(3), e2021MS002759. <https://doi.org/10.1029/2021MS002759>
- Khairoutdinov, M., Randall, D., & DeMott, C. (2005). Simulations of the atmospheric general circulation using a cloud-resolving model as a superparameterization of physical processes. *Journal of the Atmospheric Sciences*, *62*(7), 2136–2154. <https://doi.org/10.1175/jas3453.1>
- Khairoutdinov, M. F., & Randall, D. A. (2003). Cloud resolving modeling of the ARM summer 1997 IOP: Model formulation, results, uncertainties, and sensitivities. *Journal of the Atmospheric Sciences*, *60*(4), 6072–6625. [https://doi.org/10.1175/1520-0469\(2003\)060<0607:crmta>2.0.co;2](https://doi.org/10.1175/1520-0469(2003)060<0607:crmta>2.0.co;2)
- Kim, D., Jang, Y.-S., Kim, D.-H., Kim, Y.-H., Watanabe, M., Jin, F.-F., & Kug, J.-S. (2011). El Niño–Southern Oscillation sensitivity to cumulus entrainment in a coupled general circulation model. *Journal of Geophysical Research*, *116*(D22), D22112. <https://doi.org/10.1029/2011JD016526>
- Kim, D., Kug, J.-S., Kang, I.-S., Jin, F.-F., & Wittenberg, A. T. (2008). Tropical Pacific impacts of convective momentum transport in the SNU coupled GCM. *Climate Dynamics*, *31*(2–3), 213–226. <https://doi.org/10.1007/s00382-007-0348-4>
- Kooperman, G., Pritchard, M., Burt, M., Branson, M., & Randall, D. (2016). Robust effects of cloud superparameterization on simulated daily rainfall intensity statistics across multiple versions of the Community Earth System Model. *Journal of Advances in Modeling Earth Systems*, *8*(1), 140–165. <https://doi.org/10.1002/2015MS000574>
- Krishnamurthy, V., Stan, C., Randall, D. A., Shukla, R. P., & Kinter, J. L., III. (2014). Simulation of the South Asian monsoon in a coupled model with an embedded cloud-resolving model. *Journal of Climate*, *27*(3), 1121–1142. <https://doi.org/10.1175/jcli-d-13-00257.1>
- Kuo, Y., Neelin, J. D., & Mechoso, C. R. (2017). Tropical convective transition statistics and causality in the water vapor–precipitation relation. *Journal of the Atmospheric Sciences*, *74*(3), 915–931. <https://doi.org/10.1175/jas-d-16-0182.1>
- Li, F., Rosa, D., Collins, W. D., & Wehner, M. F. (2012). “Super-parameterization”: A better way to simulate regional extreme precipitation? *Journal of Advances in Modeling Earth Systems*, *4*(2), M04002. <https://doi.org/10.1029/2011MS000106>
- Lin, L., Fu, Q., Liu, X., Shan, Y., Giangrande, S. E., Elsaesser, G. S., et al. (2021). Improved convective ice microphysics parameterization in the NCAR CAM model. *Journal of Geophysical Research: Atmospheres*, *126*(9), e2020JD034157. <https://doi.org/10.1029/2020JD034157>
- Lin, Y., Dong, W., Zhang, M., Xie, Y., Xue, W., Huang, J., & Luo, Y. (2017). Causes of model dry and warm bias over central U.S. and impact on climate projections. *Nature Communications*, *8*(1), 881. <https://doi.org/10.1038/s41467-017-01040-2>
- Luo, Z., & Stephens, G. L. (2006). An enhanced convection–wind–evaporation feedback in a superparameterization GCM (SP-GCM) depiction of the Asian summer monsoon. *Geophysical Research Letters*, *33*(6), L06707. <https://doi.org/10.1029/2005GL025060>
- Moncrieff, M. W., Liu, C., & Bogenschutz, P. (2017). Simulation, modeling, and dynamically based parameterization of organized tropical convection for global climate models. *Journal of the Atmospheric Sciences*, *74*(5), 1363–1380. <https://doi.org/10.1175/jas-d-16-0166.1>
- Morrison, H. (2016). Impacts of updraft size and dimensionality on the perturbation pressure and vertical velocity in cumulus convection. Part I: Simple, generalized analytic solutions. *Journal of the Atmospheric Sciences*, *73*(4), 1441–1454. <https://doi.org/10.1175/jas-d-15-0040.1>
- Muller, C. J., Back, L. E., O’Gorman, P. A., & Emanuel, K. A. (2009). A model for the relationship between tropical precipitation and column water vapor. *Geophysical Research Letters*, *36*(16), L16804. <https://doi.org/10.1029/2009GL039667>
- Murray, F. W. (1970). Numerical models of a tropical cumulus cloud with bilateral and axial symmetry. *Monthly Weather Review*, *98*(1), 14–28. [https://doi.org/10.1175/1520-0493\(1970\)098<0014:NMOATC.2.3.CO;2](https://doi.org/10.1175/1520-0493(1970)098<0014:NMOATC.2.3.CO;2)
- Norris, J., Chen, G., & Neelin, J. D. (2019). Thermodynamic versus dynamic controls on extreme precipitation in a warming climate from the community Earth system model large ensemble. *Journal of Climate*, *32*(4), 1025–1045. <https://doi.org/10.1175/jcli-d-18-0302.1>
- Peng, L., Pritchard, M., Blossy, P. N., Hannah, W. M., Bretherton, C. S., Terai, C. R., et al. (2023). Improving stratocumulus cloud amounts in a 200-m resolution multi-scale modeling framework through tuning of its interior physics. *ESS Open Archive*. <https://doi.org/10.22541/essoar.167457989.91656039/v1>
- Petch, J. C., Blossy, P. N., & Bretherton, C. (2008). Differences in the lower troposphere in two- and three-dimensional cloud-resolving model simulations of deep convection. *Quarterly Journal of the Royal Meteorological Society*, *134*, 1941–1946. <https://doi.org/10.1002/qj.315>
- Peters, O., & Neelin, J. D. (2006). Critical phenomena in atmospheric precipitation. *Nature Physics*, *2*(6), 393–396. <https://doi.org/10.1038/nphys314>
- Phillips, V. T. J., & Donner, L. J. (2006). Cloud microphysics, radiation and vertical velocities in two- and three-dimensional simulations of deep convection. *Quarterly Journal of the Royal Meteorological Society*, *132*(621C), 3011–3033. <https://doi.org/10.1256/qj.05.171>
- Pritchard, M. S., Moncrieff, M. W., & Somerville, R. C. J. (2011). Orographic propagating precipitation systems over the United States in a global climate model with embedded explicit convection. *Journal of the Atmospheric Sciences*, *68*(8), 1821–1840. <https://doi.org/10.1175/2011jas3699.1>
- Randall, D., Khairoutdinov, M., Arakawa, A., & Grabowski, W. (2003). Breaking the cloud parameterization deadlock. *Bulletin of the American Meteorological Society*, *84*(11), 1547–1564. <https://doi.org/10.1175/bams-84-11-1547>
- Rasch, P. J., Xie, S., Ma, P.-L., Lin, W., Wang, H., Tang, Q., et al. (2019). An overview of the atmospheric component of the energy exascale Earth system model. *Journal of Advances in Modeling Earth Systems*, *11*(8), 2377–2411. <https://doi.org/10.1029/2019MS001629>
- Raymond, D. J., Sessions, S. L., & Fuchs, Ž. (2007). A theory for the spinup of tropical depressions. *Quarterly Journal of the Royal Meteorological Society*, *133*(628), 1743–1754. <https://doi.org/10.1002/qj.125>
- Richter, J. H., & Rasch, P. J. (2008). Effects of convective momentum transport on the atmospheric circulation in the Community Atmosphere Model, version 3. *Journal of Climate*, *21*(7), 1487–1499. <https://doi.org/10.1175/2007jcli1789.1>
- Rotunno, R., & Emanuel, K. A. (1987). An air–sea interaction theory for tropical cyclones. Part II: Evolutionary study using a nonhydrostatic axisymmetric numerical model. *Journal of the Atmospheric Sciences*, *44*(3), 542–561. [https://doi.org/10.1175/1520-0469\(1987\)044<0542:aaift>2.0.co;2](https://doi.org/10.1175/1520-0469(1987)044<0542:aaift>2.0.co;2)

- Smith, R. K., & Montgomery, M. T. (2012). Observations of the convective environment in developing and non-developing tropical disturbances. *Quarterly Journal of the Royal Meteorological Society*, 138(668), 1721–1739. <https://doi.org/10.1002/qj.1910>
- Stan, C., Khairoutdinov, M., DeMott, C. A., Krishnamurthy, V., Straus, D. M., Randall, D. A., et al. (2010). An ocean-atmosphere climate simulation with an embedded cloud resolving model. *Geophysical Research Letters*, 37(1), L01702. <https://doi.org/10.1029/2009GL040822>
- Stevens, B., Satoh, M., Auger, L., Biercamp, J., Bretherton, C. S., Chen, X., et al. (2019). DYAMOND: The Dynamics of the atmospheric general circulation modeled on non-hydrostatic domains. *Progress in Earth and Planetary Science*, 6(1), 61. <https://doi.org/10.1186/s40645-019-0304-z>
- Sun, Y., Solomon, S., Dai, A., & Portmann, R. W. (2007). How often will it rain? *Journal of Climate*, 20(19), 4801–4818. <https://doi.org/10.1175/JCLI4263.1>
- Tang, B. H., Rios-Berrios, R., Alland, J. J., Berman, J. D., & Corbosiero, K. L. (2016). Sensitivity of axisymmetric tropical cyclone spinup time to dry air aloft. *Journal of the Atmospheric Sciences*, 73(11), 4269–4287. <https://doi.org/10.1175/JAS-D-16-0068.1>
- Thayer-Calder, K., & Randall, D. (2015). A numerical investigation of boundary layer quasi-equilibrium. *Geophysical Research Letters*, 42(3), 550–556. <https://doi.org/10.1002/2014GL062649>
- Tompkins, A. M., & Semie, A. G. (2017). Organization of tropical convection in low vertical wind shears: Role of updraft entrainment. *Journal of Advances in Modeling Earth Systems*, 9(2), 1046–1068. <https://doi.org/10.1002/2016MS000802>
- Trenberth, K. E., Dai, A., Rasmussen, R. M., & Parsons, D. B. (2003). The changing character of precipitation. *Bulletin of the American Meteorological Society*, 84(9), 1205–1217. <https://doi.org/10.1175/BAMS-84-9-1205>
- Tulich, S. N. (2015). A strategy for representing the effects of convective momentum transport in multiscale models: Evaluation using a new superparameterized version of the Weather Research and Forecast model (SP-WRF). *Journal of Advances in Modeling Earth Systems*, 7(2), 938–962. <https://doi.org/10.1002/2014MS000417>
- Tulich, S. N., Kiladis, G. N., & Suzuki-Parker, A. (2011). Convectively coupled Kelvin and easterly waves in a regional climate simulation of the tropics. *Climate Dynamics*, 36(1–2), 185–203. <https://doi.org/10.1007/s00382-009-0697-2>
- Ullrich, P. A., & Zarzycki, C. M. (2017). TempestExtremes v1.0: A framework for scale-insensitive pointwise feature tracking on unstructured grids. *Geoscientific Model Development*, 10(3), 1069–1090. <https://doi.org/10.5194/gmd-10-1069-2017>
- Ullrich, P. A., Zarzycki, C. M., McClenny, E. E., Pinheiro, M. C., Stansfield, A. M., & Reed, K. A. (2021). TempestExtremes v2.1: A community framework for feature detection, tracking, and analysis in large datasets. *Geoscientific Model Development*, 14(8), 5023–5048. <https://doi.org/10.5194/gmd-14-5023-2021>
- Wilson, P. S., & Toumi, R. (2005). A fundamental probability distribution for heavy rainfall. *Geophysical Research Letters*, 32(14), L14812. <https://doi.org/10.1029/2005GL022465>
- Wolding, B., Dias, J., Kiladis, G., Maloney, E., & Branson, M. (2020). Interactions between moisture and tropical convection. Part II: The convective coupling of equatorial waves. *Journal of the Atmospheric Sciences*, 77(5), 1801–1819. <https://doi.org/10.1175/jas-d-19-0226.1>
- Wolding, B. O., Dias, J., Kiladis, G., Ahmed, F., Powell, S. W., Maloney, E., & Branson, M. (2020). Interactions between moisture and tropical convection. Part I: The coevolution of moisture and convection. *Journal of the Atmospheric Sciences*, 77(5), 1783–1799. <https://doi.org/10.1175/JAS-D-19-0225.1>
- Wu, X., & Yanai, M. (1994). Effects of vertical wind shear on the cumulus transport of momentum: Observations and parameterization. *Journal of the Atmospheric Sciences*, 51(12), 1640–1660. [https://doi.org/10.1175/1520-0469\(1994\)051<1640:eovwso>2.0.co;2](https://doi.org/10.1175/1520-0469(1994)051<1640:eovwso>2.0.co;2)
- Yang, Q., Hannah, W. M., & Leung, L. R. (2022). Convective momentum transport and its impact on the Madden-Julian Oscillation in E3SM-MMF. *Journal of Advances in Modeling Earth Systems*, 14(11), e2022MS003206. <https://doi.org/10.1029/2022MS003206>
- Zeng, X., Tao, W.-K., Lang, S., Hou, A. Y., Zhang, M., & Simpson, J. (2008). On the sensitivity of atmospheric ensembles to cloud microphysics in long-term cloud-resolving model simulations. *Journal of the Meteorological Society of Japan*, 86A, 45–65. <https://doi.org/10.2151/jmsj.86A.45>
- Zhang, G. J., & McFarlane, N. A. (1995). Sensitivity of climate simulations to the parameterization of cumulus convection in the Canadian Climate Centre general circulation model. *Atmosphere-Ocean*, 33(3), 407–446. <https://doi.org/10.1080/07055900.1995.9649539>
- Zhang, K., Fu, R., Shaikh, M. J., Ghan, S., Wang, M., Leung, L. R., et al. (2017). Influence of superparameterization and a higher-order turbulence closure on rainfall bias over Amazonia in Community Atmosphere Model version 5. *Journal of Geophysical Research: Atmospheres*, 122(18), 9879–9902. <https://doi.org/10.1002/2017JD026576>
- Zhou, T. J., Yu, R. C., Chen, H. M., Dai, A., & Pan, Y. (2008). Summer precipitation frequency, intensity, and diurnal cycle over China: A comparison of satellite data with rain gauge observations. *Journal of Climate*, 21(16), 3997–4010. <https://doi.org/10.1175/2008jcli2028.1>